18th ESV Paper

USING PARAMETER OPTIMIZATION TO CHARACTERIZE DRIVER'S PERFORMANCE IN REAR-END DRIVING SCENARIOS

August L. Burgett
Robert J. Miller, Jr.
NHTSA Research and Development
USA
Paper Number 305

ABSTRACT

This paper describes a means of analyzing driver's performance with driving data taken from test tracks and driving simulators for vehicles encountering rear-end driving conflicts. Measures of time-to-collision and estimated closest approach appear to allow better comparison between driving conflicts and driver's responses to conflicts under different conditions. Similar methods may be applied to field operational test data for evaluation of driver characteristics and safety measures.

INTRODUCTION

This paper consolidates three aspects of the art-and-science of describing the crash avoidance performance of motor vehicle drivers. The first aspect is the recognition that drivers utilize a two-stage process when responding to situations with the potential of producing a crash – the threat management stage followed by the maintenance stage. The second aspect is the methodology for creating parametric estimates of driver's performance during the first stage, described as the threat management stage. The third aspect is an example of the uses of the parametric description to assess driver's performance. The paper includes examples that demonstrate the two-stage braking process. It draws the conclusion that a segment of time that extends two seconds beyond the time of maximum braking by the following-vehicle captures driver's performance during the threat management stage. Finally, the paper demonstrates that the distribution of effective closest approach is a good measure of the likelihood of a crash for a given situation.

Test-track data from the CAMP project [1] is chosen to demonstrate an estimation method for all recorded driving signals. This estimation of parameters is based on a multivariate, non-linear regression procedure generally outlined in the references [2, 3, 4]. Optimized, best-fit results are obtained on driving data from a large portion of the sample database. These results of driver's reactions are subsequently analyzed with the use of the concept of a crash prevention boundary [5, 6] to provide an improvement in understanding driver's performance.

Characterizing Rear-End Driving Scenarios

A typical rear-end driving scenario is defined as one where a lead-vehicle in the same lane brakes or is moving so slowly that it presents a driving conflict for the following-vehicle driver. Realizing the conflict, the following-vehicle driver, after a short time delay to decide, brakes and/or steers in order to avoid a crash. Prior to the following-vehicle braking, the range (distance between the two vehicles) is decreasing as a function of time causing a negative range rate, dR/dt, as the two vehicles are closing on each other. Depending on the degree and timing of the driver's response there are two projected outcomes of the driving conflict and the ensuing response: either a) the following-vehicle stops first or b) the lead-vehicle stops first.

Scenario I – Following-Vehicle Stops First

Consider an example of lead-vehicle braking where the following-vehicle stops first. In Figure 1(a) a driving conflict is presented by the lead-vehicle deceleration at a constant level of 0.3 g starting at time zero (point 1). Then at point 2 the following-vehicle brakes at a sufficiently high level (0.6 g after 3.5 sec.) to avoid a crash. At 5.8 seconds into the scenario (point 3) the range begins to increase showing that the two vehicles have begun to separate. Following this, it can be seen that the following-vehicle comes to a stop (point 4) while the lead-vehicle is still moving. At the point of closest approach (point 3), range between the two vehicles was equal to 30 feet as shown by the Range-Rate by Range plot of Figure 1(b). Closest approach here is used to refer to that point where the two vehicles are at a minimum distance from each other for the driving scenario. The relevant points in time from the time plot of Figure 1(a) are also shown in the Range Rate/Range trajectory. Had the following-vehicle driver responded differently, e.g. applying only 0.4g after 3.5 sec., there would have been a collision resulting from the driving conflict. This type of response is shown by the theoretical Range-Rate/Range trajectory in Figure 2.

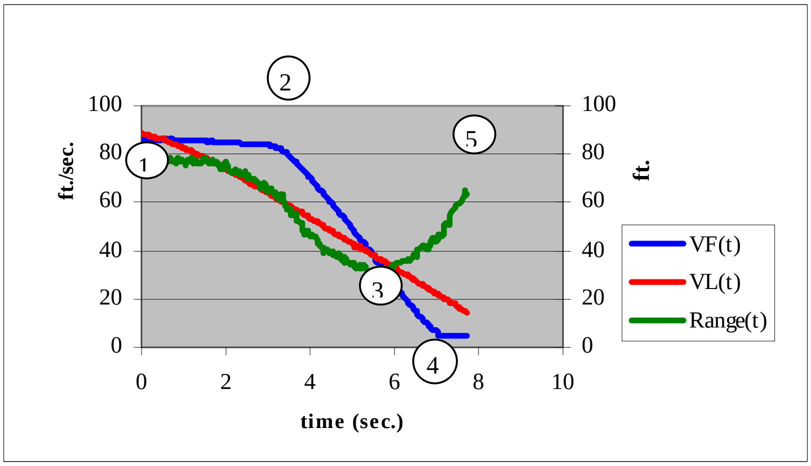

Figure 1(a). Time Plot Where Following-Vehicle Stops First.

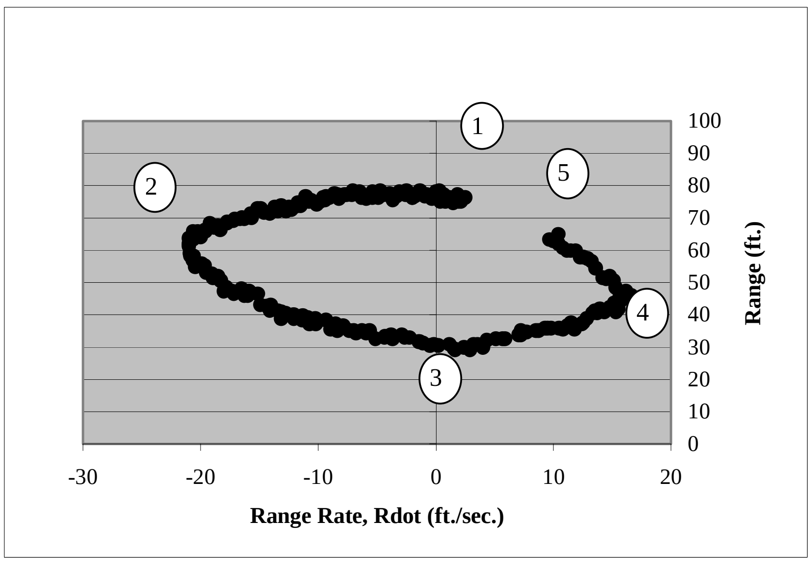

Figure 1(b). Phase Plot Where Following-Vehicle Stops First.

Figure 2. Phase Plot Where A Crash Results.

Thus, the end result of the following-vehicle reaction to a conflict as shown by the theoretical Range-Rate/Range trajectory shows whether there was a crash, a near miss, or a safely managed driving situation; and this final result has also been used as a method of classifying both the pre-crash conflict conditions and the driver's response to those conditions.

Scenario II – Lead-Vehicle Stops First

Consider another scenario as shown in Figure 3, where the lead-vehicle stops first. To begin the scenario, the lead-vehicle brakes at a constant level of 0.4g. The following-vehicle responds by braking at approximately 1.6 seconds (point 1). Later (point 2) the braking response is reduced as shown by the non-linearity in the $V_F(t)$ and the Range(t) curves as well as the Range-Rate/Range trajectory. The following-vehicle driver successfully managed the conflict between points 1 and 2 but then reduced braking between points 2 and 3 after the situation was brought under control. At point 3 (4 seconds) into the scenario, the driver resumed braking to further manage the situation during which time the lead-vehicle stopped at 5.8 seconds; and then the following-vehicle stopped at 6.1 seconds (point 4). In this driving scenario the following-vehicle stopped at a closest approach of approximately 13 feet to the lead-vehicle.

As demonstrated by the previous scenario, the following-vehicle driver will often brake in an uneven fashion in order to manage a conflict. This uneven braking has heretofore been difficult to describe in a general way. The approach in most cases has been to assume a constant value for following-vehicle braking that begins at a specific time after the initiation of a driving conflict and ends at the end of the scenario.

Characterizing Driving Scenarios Using Optimization

From the two examples in the preceding section, it can be seen that driver's response follows broad patterns associated with decelerating lead-vehicles, but there is a wide range of variation in the details of the braking response. One way of simplifying this picture is to have a parametric characterization of the motion of both vehicles. The means of characterization used in this paper is to describe the deceleration of each vehicle during the threat management stage by two parameters: the time at which effective deceleration begins and the level of deceleration. The level of deceleration is considered to be a constant-but only for a well-defined period of time. It is important to note from the outset that such characterization describes the threat management, or crash prevention, performance but does not necessarily describe the performance throughout the entire event. Thus, extrapolations of vehicle motion beyond the threat management stage may not match actual vehicle motions. The process used to establish the most appropriate value as a function of time for each of four key driving parameters is described in the following paragraphs.

An optimization process was chosen that uses a parameterized model of driver's performance and determines the best values for the parameters. This process is based on a non-linear regression approach by Marquardt [2] and others [3,4]. For the purpose here, the optimization process is adapted to a rear-end driving scenario as a function of time from beginning to end including kinematics and driver's responses. The initial, pre-crash conditions, the following-vehicle driver's response time and braking level, the closest approach of the two vehicles, and the definition of the beginning and the end of the scenario must all be considered as part of the optimization process**.**

The cornerstone of any parameter optimization process is creation of a function that measures the goodness of fit between the actual variables (such as velocities and positions) of vehicle motion and the estimates that result from the parametric characterization of motion. In this paper, a function that utilizes the difference between actual and estimates of each velocity and the difference between actual and estimate of distance between the two vehicles (Range) is used. The sum of the squares of the error function (SSE) for a scenario is given by the following expression (for $0 < t < T$, the integration interval):

$$SSE = \int_0^T [(V_{Lexp} - V_{Lopt})^2 + (V_{Fexp} - V_{Fopt})^2 + (R_{exp} - R_{opt})]^2 \, dt$$

where:
T is the upper limit of integration,
V_{Lexp} is the experimental value of lead-vehicle velocity,
V_{Lopt} is the optimized value of lead-vehicle velocity,
V_{Fexp} is the experimental value of following-vehicle velocity,

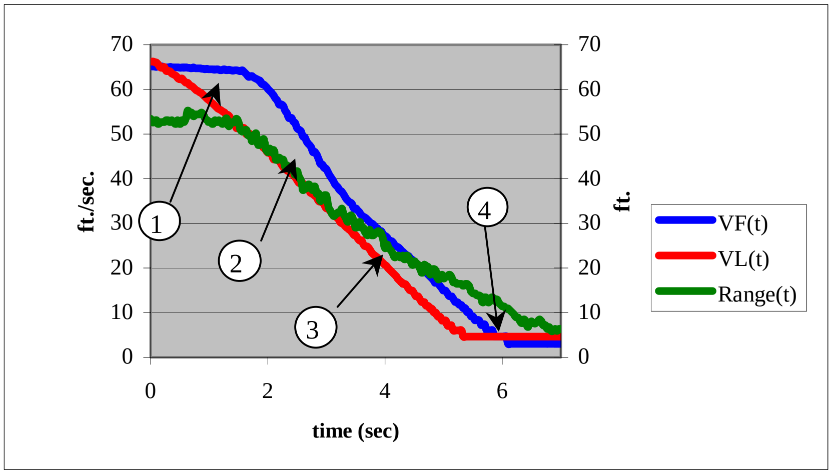

Figur 3(a). Time Plot Where Lead-Vehicle Stops First.

Figure 3(b). Phase Plot Where Lead-Vehicle Stops First.

V_{Fopt} is the optimal value of following-vehicle velocity,
R_{exp} is the experimental value of distance between the two vehicles, and
R_{opt} is the optimal value of distance between the two vehicles,

The variables $\mathbf{V_{Lexp}}$, $\mathbf{V_{Fexp}}$, and $\mathbf{R_{exp}}$ are variables derived from the experimental data. The variables $\mathbf{V_{Lopt}}$, $\mathbf{V_{Fopt}}$, and $\mathbf{R_{opt}}$ are computed estimates based on the optimizer's trial values of driver's braking time and constant level of deceleration, which are similarly based on experimental values. The form of this function emphasizes the importance of accurately matching the velocities of each vehicle as well as the distance between the two vehicles throughout the threat management stage.

As such, the parameter optimization process consists of an iterative calculation to minimize the value of SSE for different estimates of the four parameters. The value of each parameter is adjusted between iterations by an minimization algorithm that methodically produces a lower value of SSE at each iteration.

At the beginning of each iteration, the approximate values of $\mathbf{V_{Lopt}}$, $\mathbf{V_{Fopt}}$, and $\mathbf{R_{opt}}$ are reset equal to the actual values of each variable at time zero. A typical rear-end driving scenario was used to evaluate the Excel minimization algorithm (Solver) to examine the possibility of several local minima rather than one global minimum for the four-dimensional function (SSE, tFb, dF, and dL). Appendix A shows the result of this analysis to reveal one global minimum for this type of function.

Constraints forced on the optimizer solution are that deceleration values, dF and dL, are constant for the optimization period, T; and that T extends only a fixed amount beyond the peak experimental value of dF. The actual value of T will be determined by iterative trials on large data sets. Assumed constant values of deceleration for the period T allows a straightforward description of the final driver's response as is described later.

Refinement of the Optimization Process Using Experimental Data

The purpose of the parameter optimization process is to establish a parametric description of the driver's performance during the threat management stage of response. Thus, it is important, as part of the optimization process, to establish the time segment of driver's response that corresponds to the threat management stage. The integration interval, T, is the mechanism for establishing this segment of the response. At a minimum, T needs to be sufficiently long to include the time at which maximum braking of the following-vehicle occurs. However, if the value of T is too large the integration interval will extend into the second stage of driver's performance and resulting values of computed deceleration will be lower. To determine if an integration period that extends beyond this point of maximum braking is needed, an exploratory study was conducted using a variable optimization time for each driving scenario as well as a fixed optimization time.

Optimization, Using a Varying Time Interval

In the first approach, the integration interval, T, was varied beyond the peak braking response for a increasing increments of time. This approach is based on observation of the fact that the following-vehicle braking response generally rises to a peak value and then stays nearly flat or drops off rapidly as shown in Figure 4(a). In this example the following-vehicle braking profile (dF) starts at point 1 (2.5 sec.), reaches a peak at point 2 (3.8 sec.), then drops to a minimum at point 3 (5.8 sec.), and reaches a secondary peak at point 4 (9.03 sec.). These points are reflected in the phase plot of 4(b) where Rdot reaches a maximum of approximately –1.5 ft./sec shortly after point 2. Between points 1 and 2 the driver appears to brake enough to be able to manage the situation. From points 2 to 3 braking is reduced until point 3 where braking is reapplied. Point 3 is the beginning of stage two of the driver's response. This follows the threat management stage and is the stage where the driver modulates braking to achieve the desired final position of the vehicle.

A scenario with a braking response that has a quick rise time and drop off, such as shown in Figure 4, looks as if it could be optimized easily within one second after the point of maximum braking.

The test track data used for development of the parameter optimization process was created during a project that was performed by the Crash Avoidance Metrics Partnership (CAMP)[1]. These data consisted of a series of rear-end braking experiments generated on a controlled environment test track. The lead-vehicle was designed to brake at a three different constant levels for different experiments. Instrumentation for the lead-vehicle attempted to keep the deceleration level constant for a particular experiment. The following-vehicle drivers were given two specific types of braking instructions in the face of the braking lead-vehicle – hard braking and normal braking (no warning equipment was used). In the hard or "last-second" braking experiments, the following-vehicle drivers were instructed to "wait to brake until the last possible moment in order to avoid colliding with the lead-vehicle which was slowing [down]." In the normal braking experiments drivers were instructed to brake as they normally would in ordinary driving as necessary to avoid a crash with the lead-vehicle. In both braking groups, no instructions were given other than those related to braking.

The database contains approximately 1900 scenarios. In these scenarios the beginning time (lead-vehicle brake initiation) and other features of driver's performance are well documented. Optimization was performed on the entire CAMP database of normal and hard braking experiments using a variable optimization time, T, and the constraint that the difference between the actual closest approach from experimental data and the estimate of closest approach from optimized values (the ECA error) was no greater than 6.5 ft. The value of T was increased in steps until the ECA error was less than 6.5 ft. Estimated Closest Approach is defined as the minimum value of Range between the two vehicles for a given scenario.

Figure 5 shows the result of ECA comparisons of normal and hard braking data from CAMP data after optimization using the 6.5 ft. constraint. The

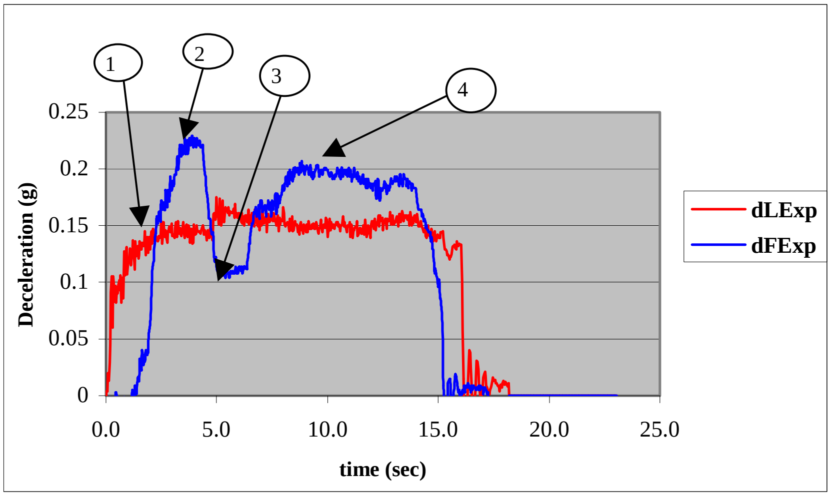

Figure 4(a). Time Plot of Braking Profiles.

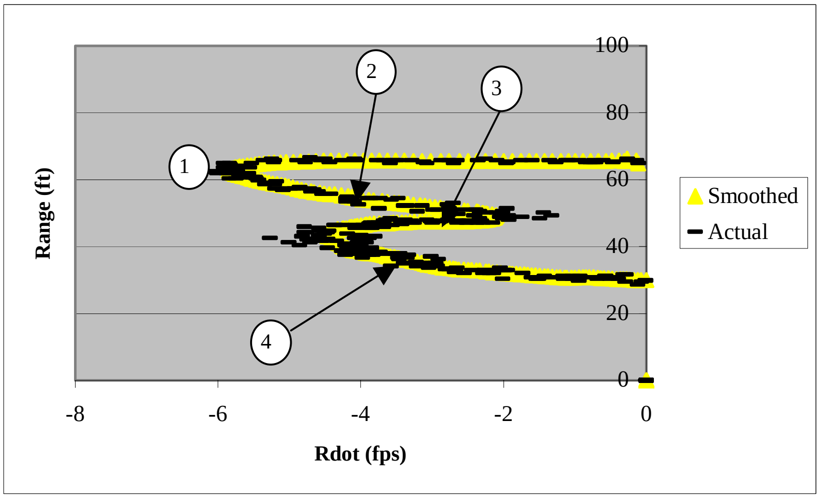

Figure 4(b). Phase Plot Reflecting Braking Profiles

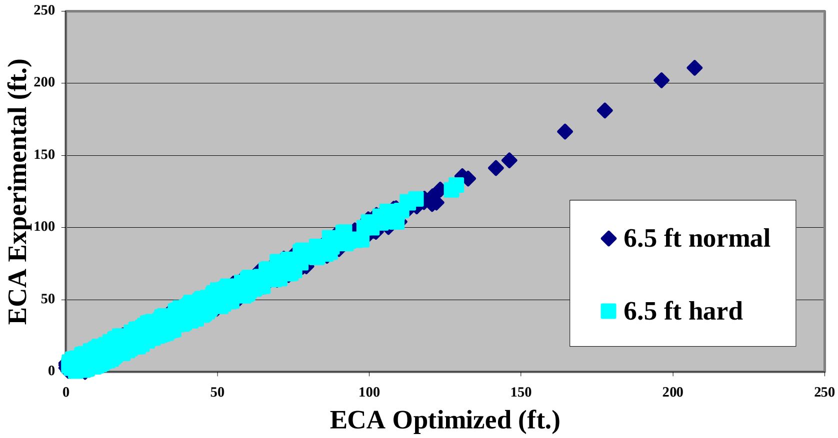

Figure 5. Estimated Closest Approach for Variable Time Interval.

histogram in Figures 6(a) also shows the cumulative distribution of the ECA error for normal braking. Note that the value of T for the first optimization cycle is the time at maximum braking. From the cumulative distribution of Figure 6 it can be seen that about 80 percent of the events had ECA error less than the 6.5 ft. condition. This means that for those events, the value of the difference between actual closest approach and approximated closest approach was less that 6.5 ft for the initial value of integration interval, i.e. T = tFb. For the other 20 percent of events, additional time beyond T = tFb was needed to satisfy the 6.5 ft condition. This means that an integration interval of peak following-vehicle braking will suffice for most optimization cases for these data. In Figure 6(b) for hard braking, a similar distribution of ECA error is shown. The distribution comparison of normal and hard braking of the time between the length of the integration interval and the time at maximum braking is shown in Figure 7.

This analysis shows that there is benefit in using an integration interval that extends beyond the point of maximum braking by the following-vehicle. However, in most cases drivers will not be trying to avoid the second stage of normal driving as they were in the CAMP experiment. Thus, a computational procedure such as the one just described that compares actual and approximate closest approach is not applicable. For these reasons, a second analysis was done in which two values of integration interval were used: T = tFb + 1 and T = tFb +2.

Optimization Using A Fixed Time Interval.

In this analysis, estimated closest approach (ECA) was again used as the metric for comparison of each scenario of the CAMP data. Comparisons of the optimized closest approach vs. the actual closest approach for the two intervals are given in Figures 8(a) and 8(b) for normal and hard braking; and these figures show a much wider variation in ECA error due to the removed constraint. The cumulative distributions of actual minus optimized ECA are shown in Figures 9(a) and 9(b) for normal and hard braking respectively. Based on the information in Figure 9, it was decided that a value of T = tpb + 2 sec would be used for the analysis of data described in the next section.

Example of Optimization

As an example of application of a parameter optimization process using a fixed interval, Figure 10 below with five frames (10a thru 10e) shows the experimental input functions and the optimized results of a typical hard braking rear-end CAMP experiment. The first frame of the figure, 10(a), shows the input experimental data for velocities and range over the full experiment period. The second frame of the figure, 10(b), shows the optimized results of the same data for comparison. Frame 10(c) shows braking profiles for both experimental and optimized data. A range/range rate plot in frame 10(d) replots both experimental and optimized data with time as a parameter. Frame 10(e) is a crash prevention boundary (CPB) [5] plot based on the optimized parametric description of driver's response. In the above case the optimization period used was from zero to 7.03 due to the fact that the peak value of dF occurred at 5.03 seconds. This example demonstrates the use of the optimizer to obtain the driver's performance metrics from measured inputs in a typical CAMP driving experiment.

<u>Applications</u>

In this section, the parameter optimization process developed in the preceding sections is applied to two sets of experimental data. The first set comes from an experiment in which a driving simulator was used to test driver's response to impending rear-end crashes [7]. In this experiment, the drivers were provided with an imminent crash warning for a subset of trials and did not have such a warning for a second subset. A second set of data is from the previously mentioned CAMP test track experiment in which drivers were exposed to sudden deceleration by a preceding vehicle. In one subset of the experiment, drivers were instructed to brake normally while in a second subset they were instructed to wait until the "last second" before braking. The simulator data also shares the common feature that it has two subsets; one of which represents a more hazardous driving situation than the other.

By way of background, the previously referenced tool for analyzing driver's performance in situations such as those described above, called the crash prevention boundary (CPB) was introduced in 2001 [5]. The concept behind the CPB is that there is an analytically definable line that separates driver's performance that prevents a crash from driver's performance that does not prevent a crash. A sample CPB is shown in Figure 11. In reference [5] each run from the driving simulator experiment was analyzed using a CPB framework without the optimization process. Each CPB had a specific set of initial conditions of deceleration, range, and velocity as

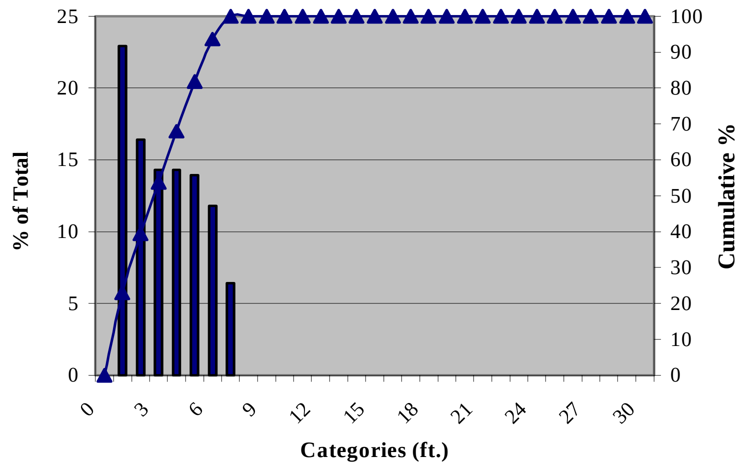

Figure 6(a). ECA Error, Variable Time Interval for Normal Braking.

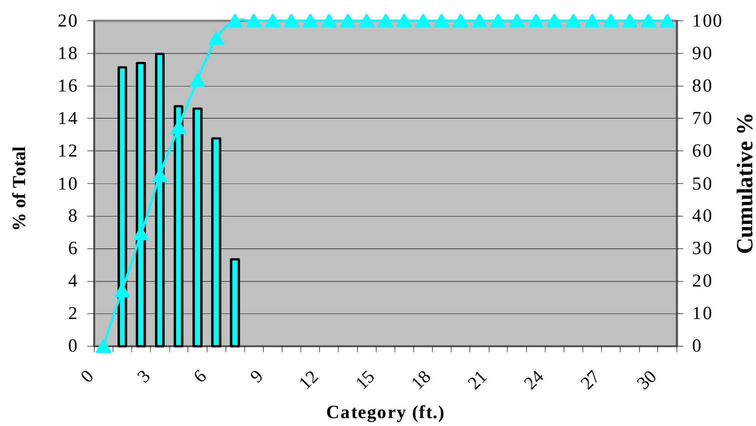

Figure 6(b). ECA Error, Variable Time Interval for Hard Braking.

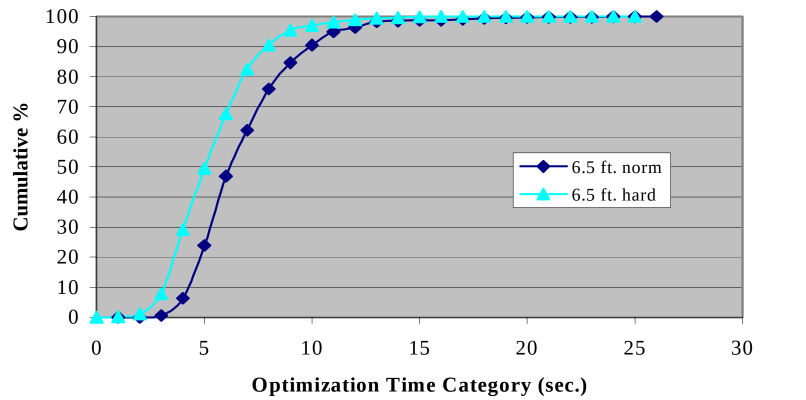

Figure 7. Optimization Time Comparisons.

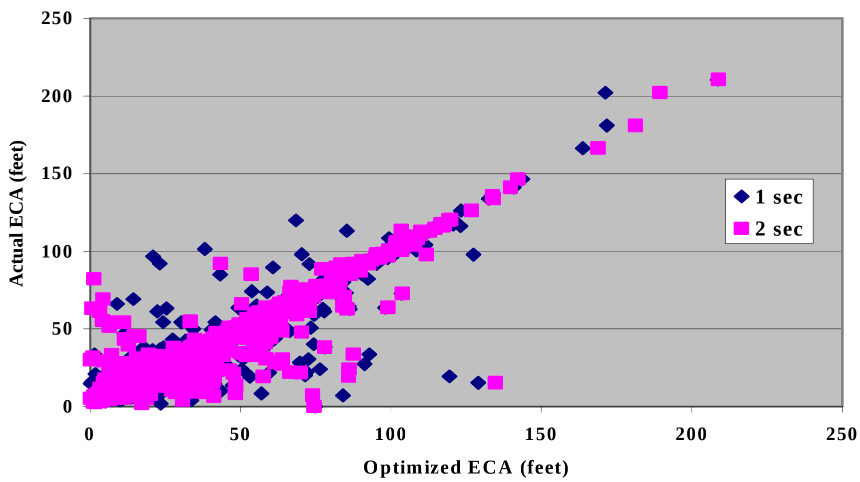

Figure 8(a). ECA Comparison for Fixed Optimization Periods and Normal Braking.

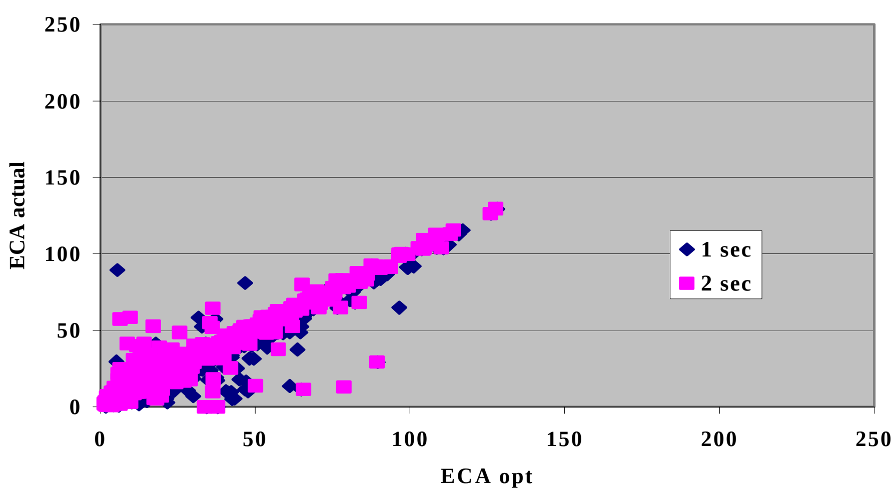

Figure 8(b). Estimated Closest Approach for Fixed Optimization Periods and Hard Braking.

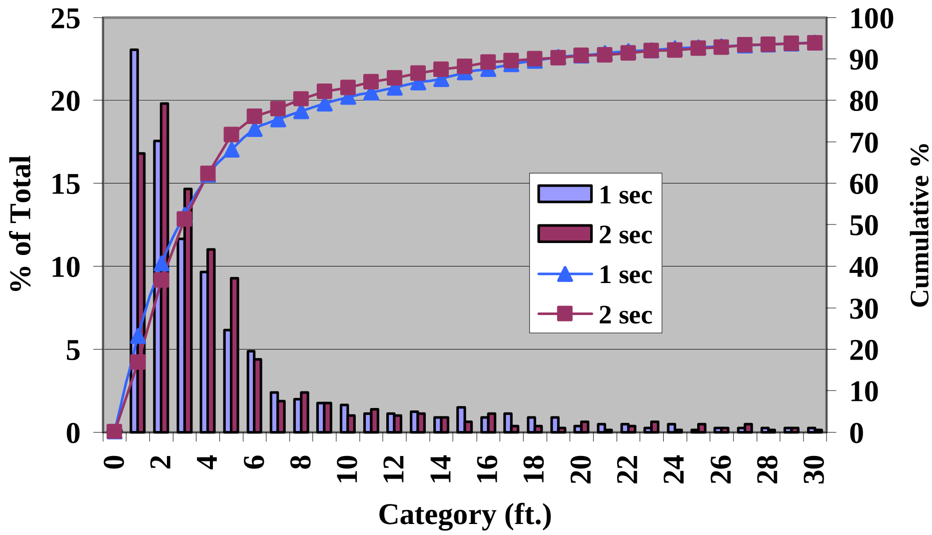

Figure 9(a). ECA Error, Fixed Optimization Times and Normal Braking.

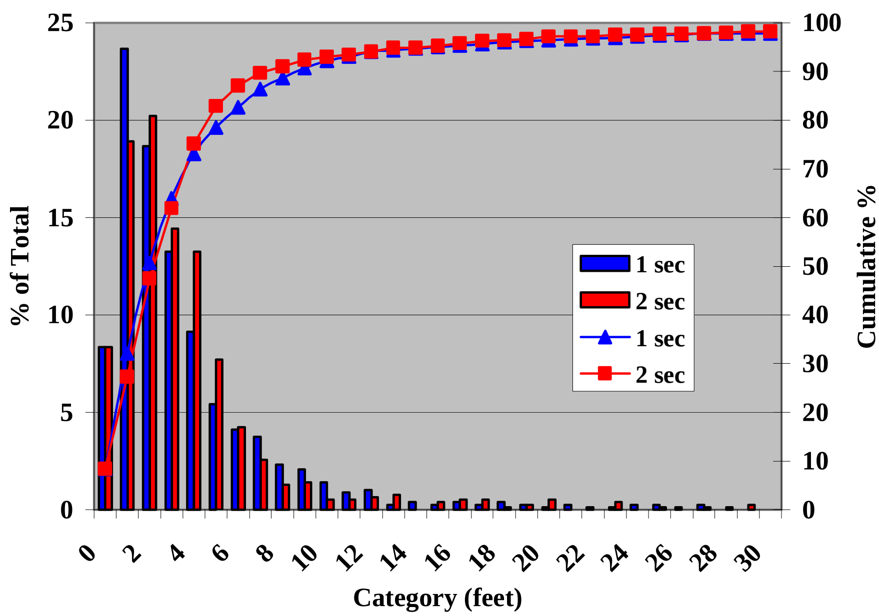

Figure 9(b). ECA Error, Fixed Optimization Times and Hard Braking.

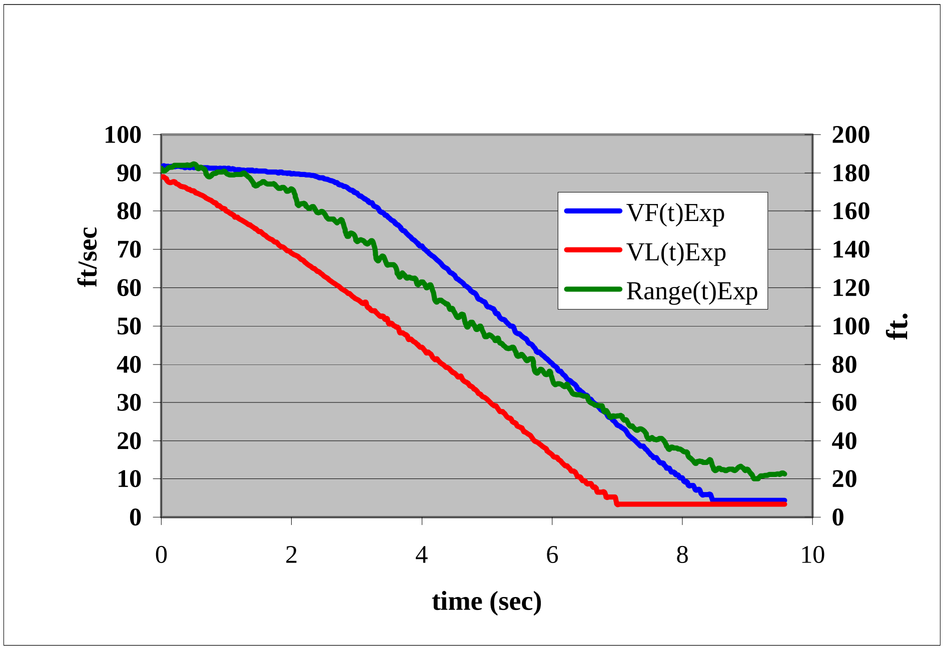

Figure 10(a). Time Plot of Experimental Velocity and Range Data.

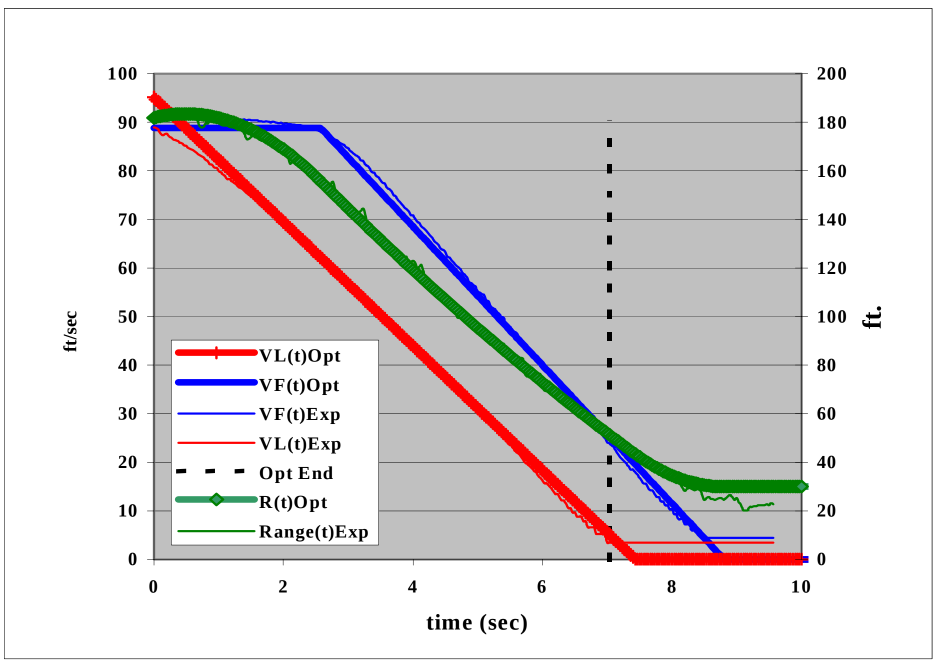

Figure 10(b). Time Plot of Experimental and Optimized Velocity and Range Variables.

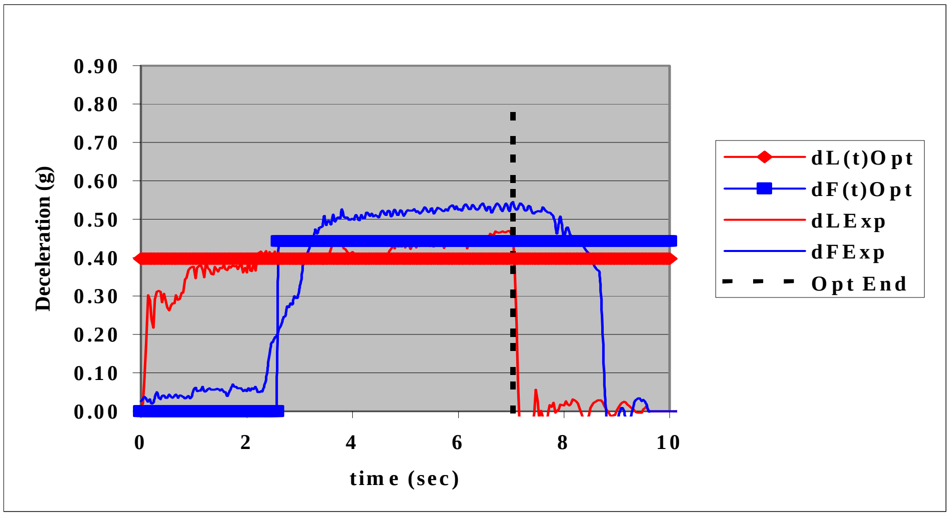

Figure 10(c). Optimized vs. Experimental Values Braking Profiles.

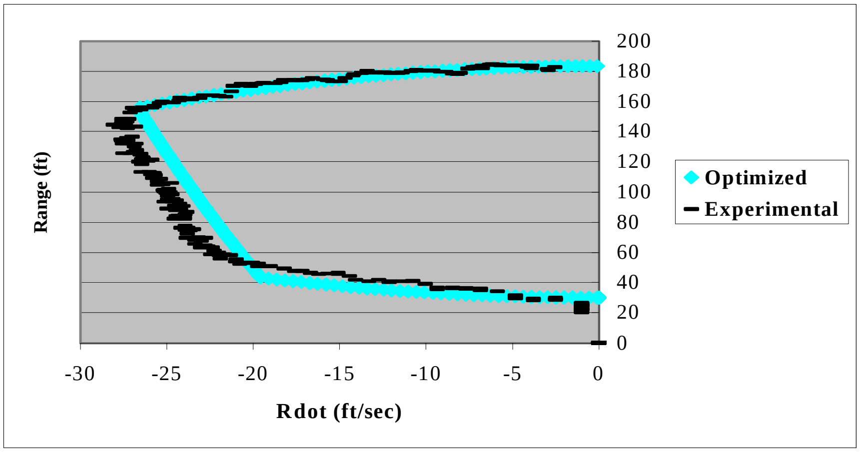

Figure 10(d). Phase Plane Plot of Optimized vs. Experimental Data.

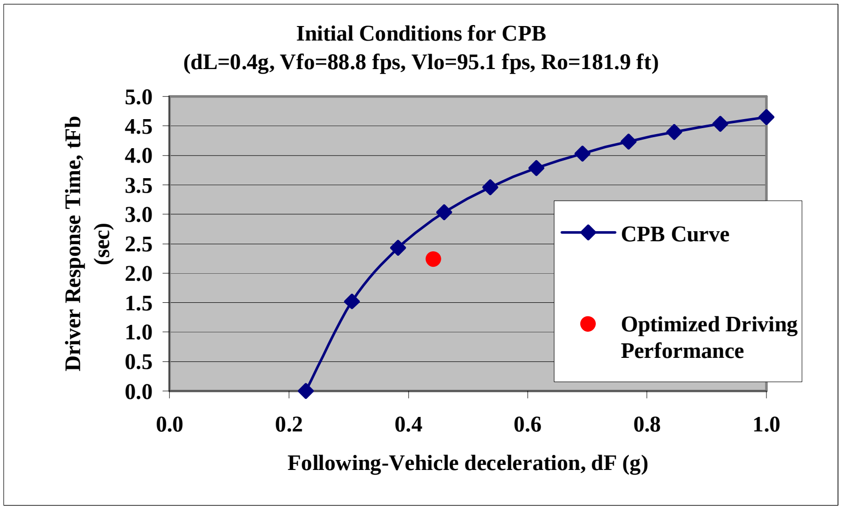

Figure 10(e). Crash Prevention Boundary with Driver's Response.

defined by the test conditions. It was seen that driving responses leading to a crash fell on one side of the CPB; and driving responses leading to a non-crash fell on the other side of the CPB. An extension of the CPB concept is observing the closeness of the driver's response to the CPB curve, i.e. the distance between the driver's performance in a situation and the CPB for that situation would be a useful metric of the level of threat for specific situations. The estimate of closest approach (ECA) based on the optimization process during the threat management stage of driver's response is such a metric and is used for the remainder of this analysis. To illustrate this extension, lines of constant values of ECA are shown in Figure 11 along with the CPB.

Of the data to be analyzed from the driving simulator experiment [5, 7], only a single set of test conditions from that experiment is used here. The condition compares a series of runs without a warning to a series of tests with a short warning time. The best values of the parametric description of driver's performance for each run were calculated using the previously described parameter optimization process. These values were then used to calculate the ECA for each run in the data sets. The distribution of ECA for the two subsets is shown in Figure 12. Negative ECA values in Figure 11 correspond to crashes. The description of a driver's performance would appear as a point above the CPB in a diagram like Figure 11. Positive ECA values correspond to non-crashes and would appear below the CPB. From Figure 12, it is seen that the difference in the two distributions of ECA does reflect the relative hazard of the two types of driving, with an imminent crash warning and without. In those cases where the drivers had a warning, the distribution of ECA is further to the right. This indicates that these drivers were performing in a manner that produces fewer crashes. This corresponds to the location of the description of

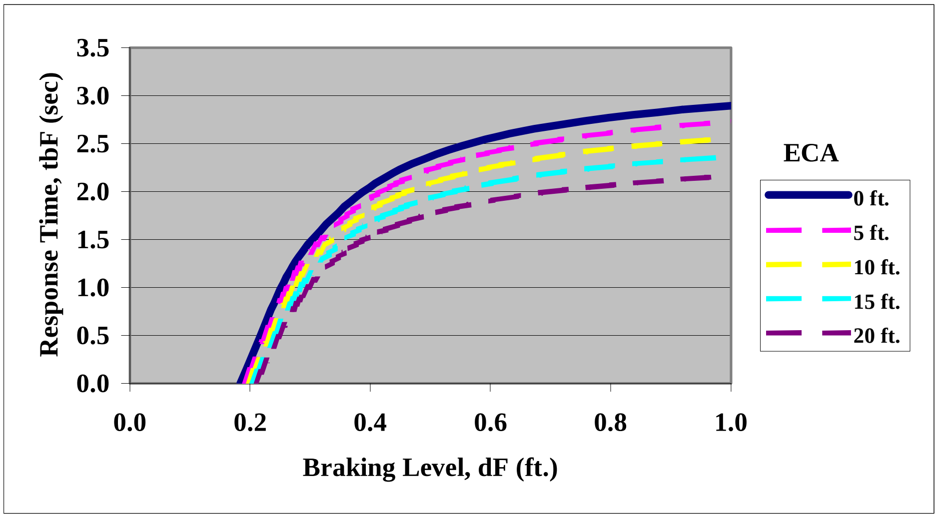

Figure 11. Various ECA Positions from a CPB Curve

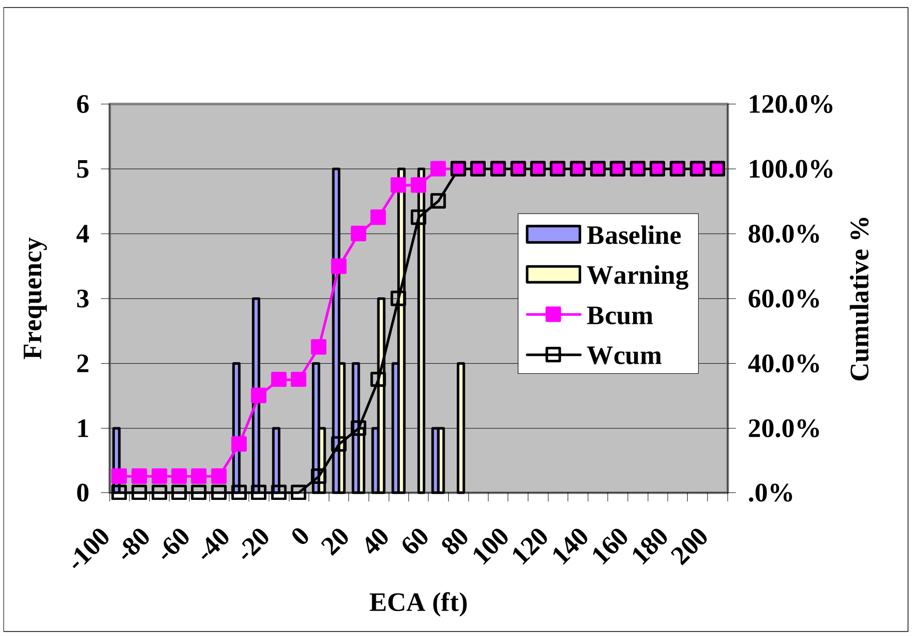

Figure 12. Simulator ECA Histogram.

the driver's performance being at a greater ECA value from the CPB.

The results of a similar analysis of the CAMP project are shown in Figure 13. The data in this figure includes the combined responses for all three levels of lead-vehicle deceleration (dL=0.15g, 0.3g, and 0.4g). It can be seen that there is a small difference in the distributions of ECA between normal braking and hard braking. As expected, the hard braking subset produces smaller values of ECA (median ECA for hard braking equals 28 ft. and median ECA for normal braking equals 33 ft.

However, as seen in Figure 14, the distribution of ECA conditions are noticeably different. In this case

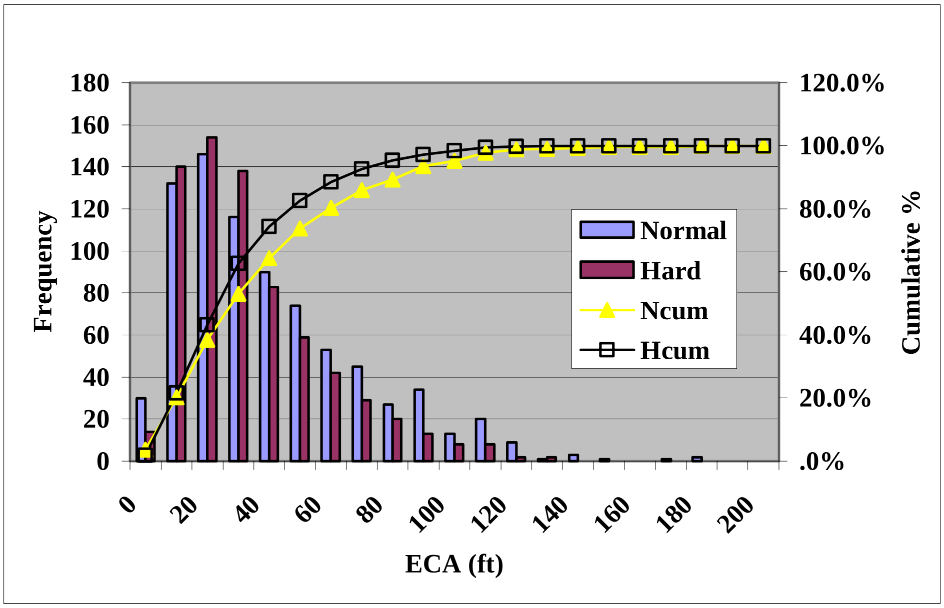

Figure 13. CAMP ECA Comparisons.

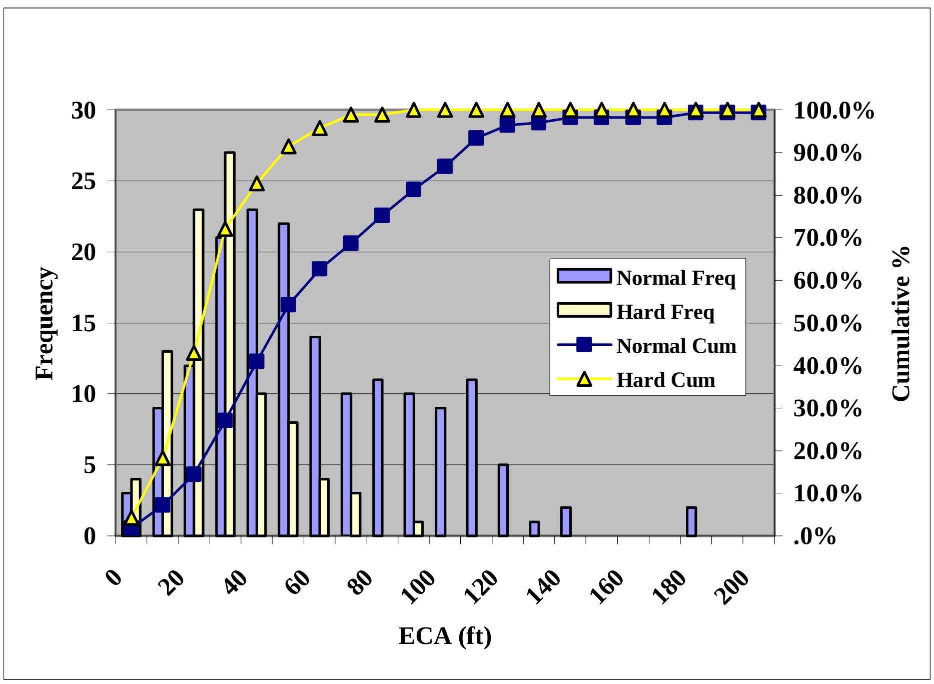

Figure 14. CAMP ECA Statistics for dL = 0.15 g

(dL=0.15g) the median value for hard braking is 28 ft. and the median value for normal braking is 52 ft. These results substantiate the conclusion from the driving simulator experiment that more hazardous conditions are reflected in ECA cumulative distributions that are farther to the left.

The results from the parameter optimization process can also be used to study other aspects of driver's performance, for example, time-to-collision (TTC) at the time of following-vehicle braking (TTCb). While ECA estimates the effect of the driver's response, TTCb estimates the situation prior to the response. For this analysis, TTC is calculated at the time that effective braking begins, as determined by the parameter optimization process.

Figure 15 shows the distribution of TTC for the two subsets of the driver simulator experiment (baseline vs. warning). It can be seen that the values of TTCb when the driver was given a warning are substantially longer than when no warning was given. Similarly, TTCb cumulative values more to the left represent a higher degree of danger than cumulative values to the right. The TTCb results for the CAMP experiment are shown in Figure 16. As for the simulator data, it is seen that the values of TTC for hard braking are substantially shorter than when drivers braked in a normal manner from cases where they waited to brake per the hard braking instruction. These curves indicate that cumulative distribution values on the

SUMMARY AND CONCLUSIONS

This paper consolidates three aspects of the art-and-science of describing the crash avoidance performance of motor vehicle drivers. The first aspect is the recognition that drivers utilize a two-stage process when responding to situations with the potential of producing a crash. The second aspect is the methodology for creating parametric estimates of driver's performance during the first stage, described as the threat management stage. The third aspect is an example of the uses of the parametric description to assess driver's performance.

Two examples of data presented herein support the suggestion that drivers respond in a two stage manner to situations with the potential of a rear-end conflict. The first stage is threat management. This is the stage that determines whether or not a crash will occur. It is further shown that a parametric description of driver's performance during the threat management stage provides a simple, but effective foundation for analyzing driver's performance in these situations. The paper then develops a consistent procedure for optimization of driving data variables to determine the best description of the driver's performance during the threat management stage of the following-vehicle driver's response. This procedure is used to analyze data sets from two experiments, one that utilized a driving simulator and a second that utilized a test track.

The major conclusion from this study is that improved understanding of how drivers avoid rear-end crashes can be obtained through the process described and developed in this paper. Quantitatively, this study shows that the distribution of the time-to-collision at following-vehicle braking is a good measure of the level of hazard of a driving situation and that estimated closest approach (ECA) is a good, single parameter measure of the driver's response to the hazardous situation.

As an example, in an experiment where some drivers were provided with an imminent crash warning and others were not, the median of the distribution of Estimated Closest Approach was 40 ft. larger for those drivers with the warning. This feature of the process outlined in this paper offers the potential for being a powerful tool for assessing the level of hazard for various driving situations and the safety impact of warnings and other crash prevention measures.

NOMENCLATURE

Actual Data: Experimentally measured data.
Baseline: Driving data derived without giving a driver a crash warning.
CPB: Crash Prevention Boundary. A hypothetical boundary that separates driver responses into crash and non-crash regions.
Cum: Abbreviation for cumulative values.
dF: Following-vehicle braking level in g's.
dL: Lead-vehicle braking level in g's.
dR/dt: The mathematical time derivative of Range. ECA: Estimated Closest Approach.
ECA: Estimated Closest Approach. A computed value of the minimum distance that two vehicles would come from each other based on known or computed values of velocity, range, and deceleration in a rear-end driving scenario.
ECA Error: Difference between optimized and experimental ECA values.
Exp: Abbreviation for Experimental values.
IDS: Iowa Driving Simulator.
Opt: Abbreviation for Optimized values.
Opt End: Optimization end time.
R(t): Range as a function of time.
Range(t): Same as R(t).
Range-Rate/Range trajectory: Locus of all points in a phase plot for a driving scenario.
Rdot: Range Rate, dR/dt.
R_{exp}: Experimental value of range.
R_{opt}: Optimized value of range.
Rear-end driving scenario: An event whereby two vehicles approach each other in the same driving lane due to the slower speed of the lead-vehicle with respect to the following-vehicle. The lead-vehicle may be traveling at a constant speed or may be decelerating.
Smoothed Data: Experimental data that is smoothed using an 11 point smoothing algorithm.

.

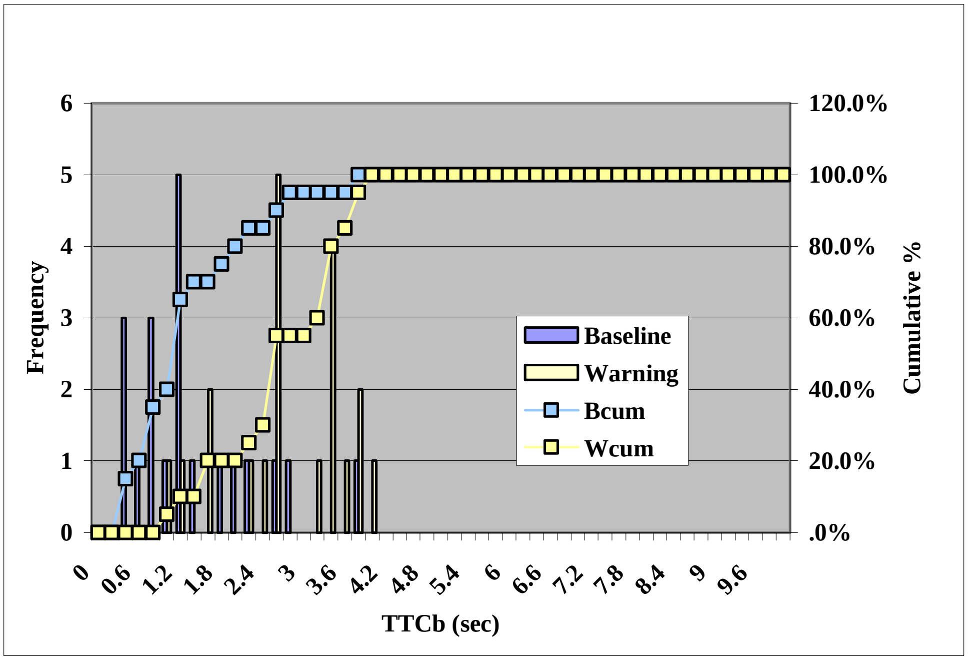

Figure 15. Histogram of Simulator TTC Values at Braking.

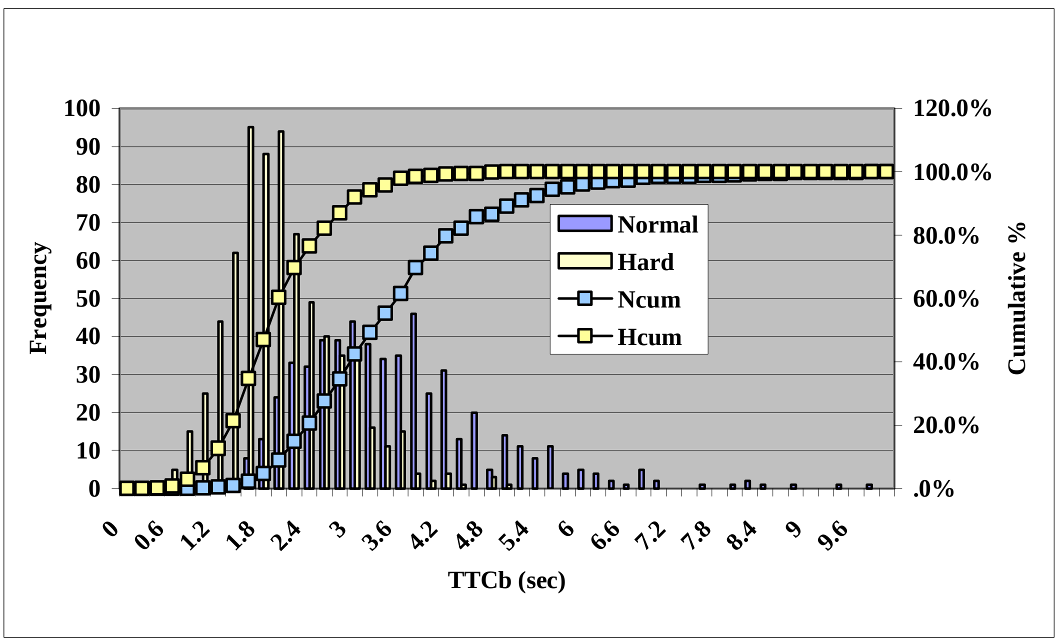

Figure 16. Histogram of CAMP TTC Values at Braking.

SSE: Sum of the squares of the errors between experimental and optimized variables T: The value of the integration interval for the SSE function.
tFb: The time of following-vehicle brake initiation.
tpb: The time of peak braking for the following-vehicle.
TTC: Time-to-collision based on no following-vehicle response.
TTCb: Time-to-collision at following-vehicle braking.
$V_F(t)$: Following-vehicle velocity as a function of time.
V_{Fexp}: Following-vehicle velocity from experimental measurements.
V_{Fopt}: Following-vehicle velocity from the optimization process.
$V_L(t)$: Lead-vehicle velocity as a function of time.
V_{Lexp}: Lead-vehicle velocity from experimental measurements.
V_{Lopt}: Lead-vehicle velocity from the optimization process.

REFERENCES

[1] Kiefer, R., LeBlanc, D., Palmer, M., Salinger, J., Deering, R., and M. Shulman. *Development and Validation of Functional Definitions and Evaluation Procedures for Collision Warning/Avoidance System*s. Report DOT HS 808 964, August 1999.

[2] Marquardt, D. W. “An Algorithm for Least Squares Estimation of Non-Linear Parameters”.” *Journal of the Society of Industrial and Applied Mathematics* 11 (1963), pp. 431-41.

[3] Dillon, W.R. and Goldstein, M. (1984), *Multivariate Analysis*, New York: John Wiley & Sons, Inc.

[4] Gnanadesikan, R. (1997), *Methods for Statistical Data Analysis of Multivariate Observations*, Second Edition, New York: John Wiley & Sons, Inc.

[5] Burgett A.L., Miller, R.J. (2001), *A New Paradigm for Rear-End Crash Prevention Driving Performance*, SAE 2001 World Congress, Detroit, Michigan, March 5-8, 2001, 2001-01-0463.

[6] Martin, P.G. and Burgett, A.L. (2001), *Rear-end Collision Events: Characterization of Impending Crashes*, Proc. of the 1st Human-Centered Transportation Simulation Conference, The University of Iowa, Iowa City, Iowa November 4-7, 2001 (ISSN 1538-3288).

[7] Lee, John D., McGehee, Daniel V., Brown, Timothy L., and Ries, Michelle L., *Driver distraction, warning algorithm parameters, and driver response to imminent rear-end collisions in a high-fidelity simulator,* The University of Iowa, July 27, 2000, Contract DTNH22-95-D-07168, IQC No. Two (8-07633).

Appendix A Solutions of the SSE Equation

In order to examine the SSE function:

$$SSE = \int_0^T [(V_{Lexp} - V_{Lopt})^2 + (V_{Fexp} - V_{Fopt})^2 + (R_{exp} - R_{opt})]^2 \, dt$$

for the location of global minima, the function was computed for incremental values of dL, dF, and tFb to determine values of VF, VL, and R to compare with actual experimental values. It is necessary to determine if the optimizer is most likely finding a unique minimum for all available minimum solutions. Solutions for SSE in one sample case as given by the equation below were then plotted as three-dimensional surfaces, one surface per constant value of dL. The values of T is constant for all solutions.

Several local minima were located for the surface where dL=0.15. The actual solution obtained by the algorithm was SSE = 16.9, for the values of dL = 0.15, tFb = 1.92, and dF= 0.21. Examination of all the other surfaces plotted for 0<dL<1.0, showed no lower minima other than that found by the optimizer. Three views of the surface for dL=0.15 are shown in Figures A-1, 2, and 3 to depict the presence of local minima in this plane. Since the character of the experimental data a reasonably uniform, it is concluded that a unique minimum is found consistently by the optimizer for these data.

Plots of the time-varying functions, both experimental and optimized, are shown in Figure A-4, 5, and 6 for the velocities, range, and displacement; the braking functions; and the Range/Range Rate plot. It should be noted that the optimization process ended 2 seconds after the experimental peak value of dF. It should also be noted that the optimized values of dF and dL are constant for the scenario.

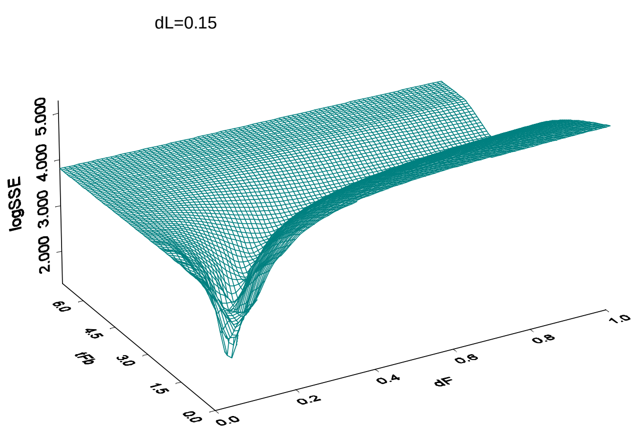

Figure A-1 Constant dL Surface.

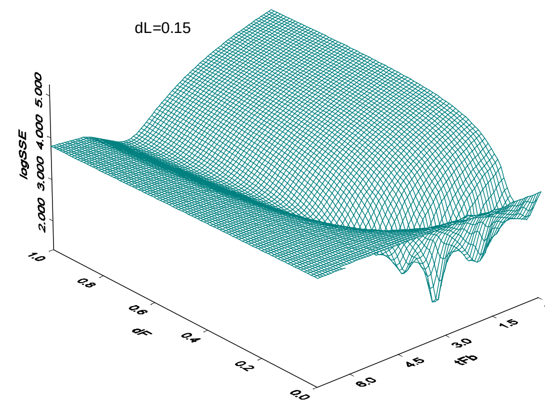

Figure A-2. Constant dL Surface Rotated CCW.

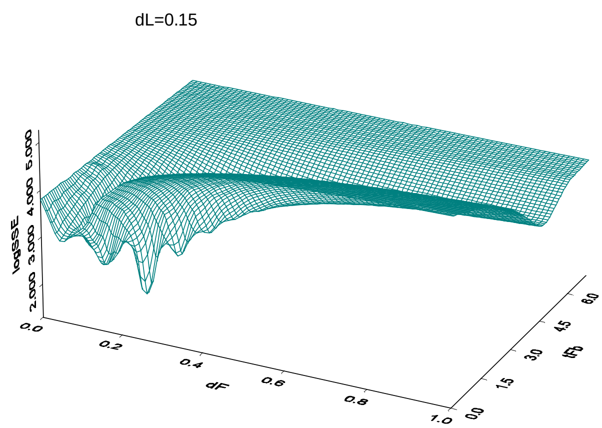

Figure A-3 Constant dL Surface Rotated CW

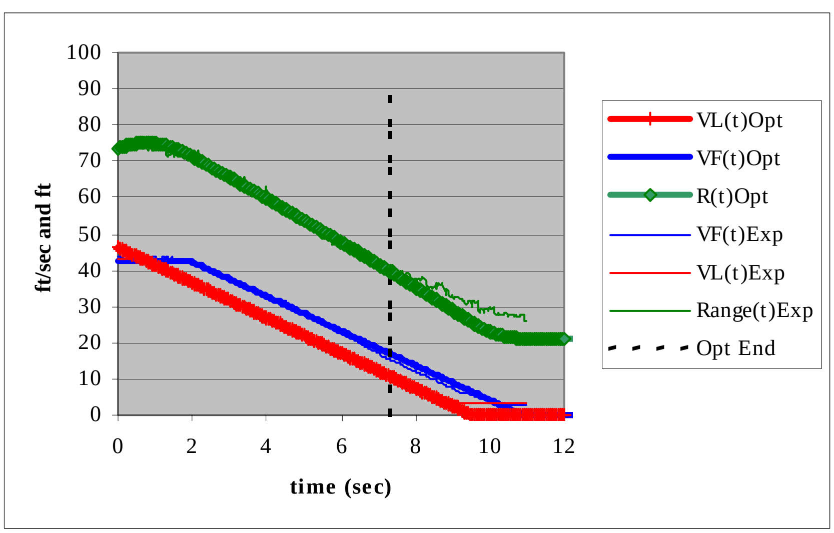

Figure A-4 Time-Varying Experimental and Optimized Functions

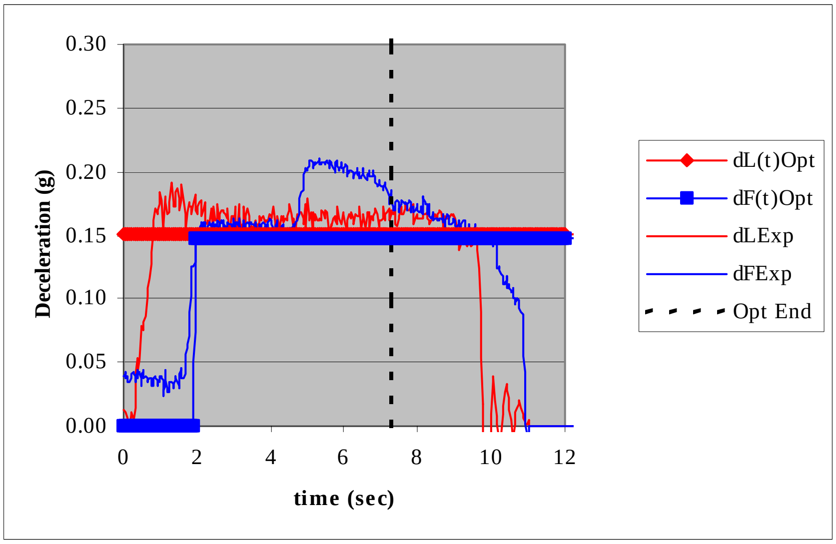

Figure A-5 Time-Varying Experimental and Optimized Braking Functions

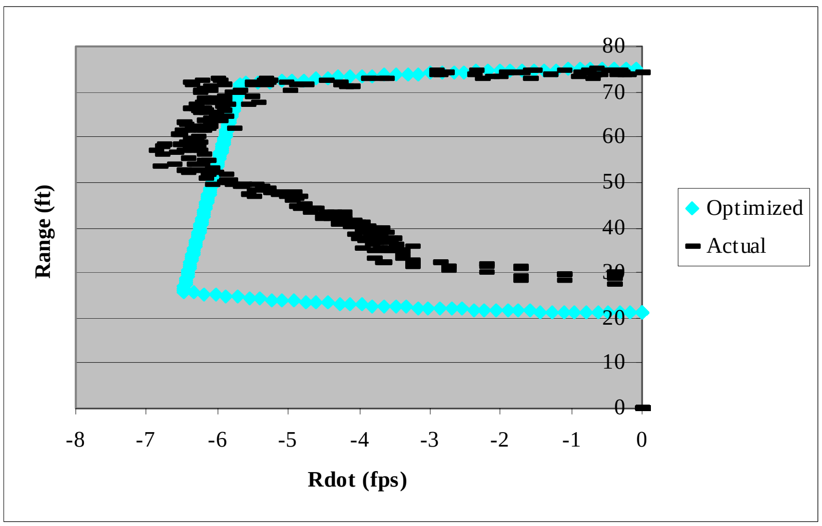

Figure A-6 Range vs. Range Rate for Experimental and Optimized Data